New insights into the thermally activated defects in *n*-type float-zone silicon

Cite as: AIP Conference Proceedings **2147**, 140014 (2019); https://doi.org/10.1063/1.5123901
Published Online: 27 August 2019

Yan Zhu, Fiacre Rougieux, Nicholas Grant, Jack Mullins, Joyce Ann De Guzman, John D. Murphy, Vladimir P. Markevich, Gianluca Coletti, Anthony R. Peaker, and Ziv Hameiri

New Insights into the Thermally Activated Defects in *n*-Type Float-Zone Silicon

Yan Zhu[1, a)] Fiacre Rougieux[1], Nicholas Grant[2], Jack Mullins[3], Joyce Ann De Guzman[3], John D. Murphy[2], Vladimir P. Markevich[3], Gianluca Coletti[1, 4], Anthony R. Peaker[3], and Ziv Hameiri[1]

[1]*University of New South Wales, Sydney, NSW 2033, Australia*
[2]*University of Warwick, Coventry, CV4 7AL, United Kingdom*
[3]*University of Manchester, Manchester, M13 9PL, United Kingdom*
[4]*ECN part of TNO, Le Petten, NL-1755, Netherlands*

[a)]Corresponding author: yan.zhu@student.unsw.edu.au

Abstract. Float-zone silicon has been long assumed to be bulk defect free and stable. Nevertheless, recently it was found that upon annealing between 450 °C to 700 °C detrimental defects can be activated in this material. Previous studies via deep level transient spectroscopy have identified several defect levels. However, it is still not clear which of these levels have a substantial impact on the minority carrier lifetime. In this study, we determine the recombination parameters of the dominant defect level using a combination of deep level transient spectroscopy and temperature and injection dependent lifetime spectroscopy. Additionally, we investigated the effect of hydrogenation on the thermally activated defects in *n*-type float-zone silicon.

INTRODUCTION

Providing high minority carrier lifetime, float-zone (FZ) silicon has been long conceived as a bulk defect lean and stable material. Therefore it is widely used in the photovoltaic community for the fabrication of high efficiency solar cells,[1,2] control wafers of various experiments,[3,4] monitoring surface passivation quality,[5,6] modeling intrinsic recombination[7] *etc.* Nevertheless, recently it was found the lifetime of FZ silicon can drop by more than two orders of magnitude after a heat treatment between 450 to 700 °C. [8,9] This severe degradation was found to be due to the activation of bulk defects during the heat treatment.[8,9] Therefore, special care is needed if the FZ silicon wafers used undergo processes in the temperature range between 450 to 700 °C. Fortunately, it was found that the thermally activated defects can be permanently deactivated after an annealing at 1000 °C for 30 mins.[8,9] It was suspected that the defects activated during the degradation are related to the nitrogen doping during crystal growth and un-clustered vacancies.[10] More recent studies reveal that FZ wafers can also degrade under light and elevated temperature.[11,12]

Deep level transient spectroscopy (DLTS) measurements from previous studies have found several defect levels in the degraded samples.[8,10] However, DLTS alone does not reveal which level is the dominant in the recombination of charge carriers. Temperature and injection dependent lifetime spectroscopy (TIDLS) is another technique widely used for defect characterization.[13,14] As it is based on lifetime measurements on bulk samples, TIDLS is more sensitive to the dominant defect levels which limit the effective lifetime of the sample. The purpose of this study is to determine the dominant recombination level in annealed FZ silicon wafers by combining TIDLS and DLTS, and to explore the effect of hydrogenation passivation on the thermally activated defects. In this work, we focus only on *n*-type FZ silicon.

SiliconPV 2019, the 9th International Conference on Crystalline Silicon Photovoltaics
AIP Conf. Proc. 2147, 140014-1–140014-6; https://doi.org/10.1063/1.5123901
Published by AIP Publishing. 978-0-7354-1892-9/$30.00

METHODS

Three groups of 4 inch diameter *n*-type FZ silicon wafers (1 Ωcm, grown in a nitrogen ambient) from the same manufacturer were prepared. Group N (**n**o anneal) contains three as-grown wafers without any thermal process. Group D (**d**egraded) contains four wafers annealed at 500 °C under nitrogen ambient for 30 mins. Group A (defect **a**nnihilated) contains three wafers annealed at 1000 °C under nitrogen ambient for 30 mins. Since the wafers may not be neighboring wafers from the same ingot, multiple wafers are used in each group to improve the statistics of the measurements.

After annealing, room temperature lifetime and photoluminescence (PL) imaging of all wafers were firstly measured by means of superacid-derived passivation [bis(trifluoromethane)sulfonimide (TFSI) in 1, 2-dichloroethane (DCE)].[15] Superacid-derived passivation provides excellent passivation quality (surface recombination velocity, SRV, around 1 cm/s) and does not add thermal budget to the samples (as it is conducted at room temperature).[15] After room temperature measurements with superacid-derived passivation, the samples then went through RCA cleaning and an amorphous silicon (a-Si) surface passivation via plasma-enhanced chemical vapor deposition (PECVD). To minimize the thermal budget on the samples, the deposition temperatures were kept below 200 °C. This a-Si layer was found to provide a stable passivation up to 200 °C with an SRV below 10 cm/s. TIDLS measurements were then performed from -50 to 150 °C using a customized quasi-steady-state photoconductance lifetime tester based on the WCT-120 from Sinton Instruments.[16] A cryostat has been incorporated into the system to enable lifetime measurements at various temperatures.

After TIDLS measurement, the a-Si layer was stripped off from the samples (a mixture of 49% hydrofluoric acid and 69% nitric acid with a ratio of 1:10 for two minutes followed by rinsing in deionized water). DLTS measurements were then performed on one wafer from each group. Schottky barrier diodes were fabricated by thermal evaporation of gold (Au) to the front surface of the samples, while ohmic contacts were fabricated by thermal evaporation of aluminum (Al) to the back surface. In order to investigate the effect of hydrogenation of the thermally-activated defects, another wafer from each group went through a silicon nitride (SiN_x) surface re-passivation via PECVD.[17] The temperature of the deposition was around 425 °C. No additional firing has been done to the samples after the SiN_x deposition.

RESULTS

Thermal Activation of the Defects

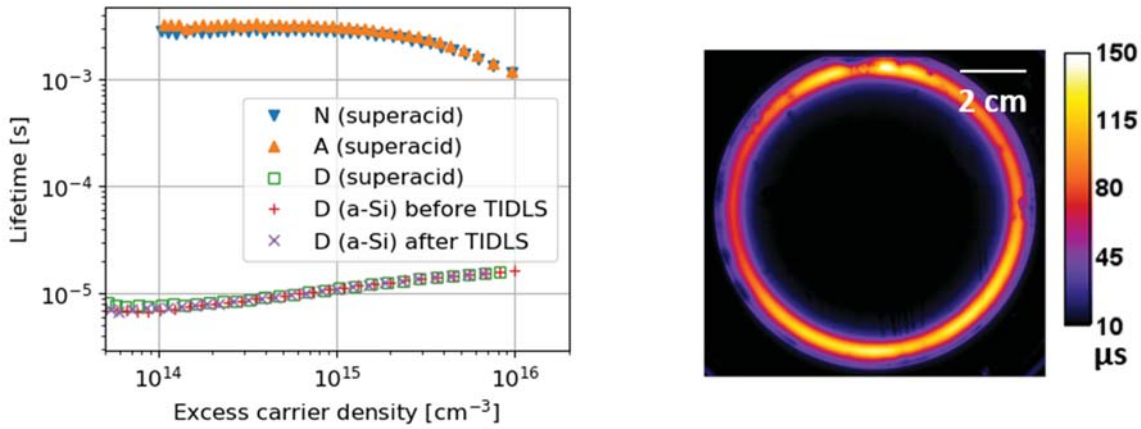

(a) (b)

FIGURE 1. (a) Room temperature injection dependent lifetime curves of the 1 Ωcm *n*-type FZ-Si samples with superacid-derived passivation in the unannealed state ("N") and defect annihilated state ("A") as well as the room temperature lifetime of the degraded sample ("D") with a-Si passivation before and after the TIDLS measurements. (b) PL image of the degraded sample ("D") after the superacid-derived passivation.

Room temperature injection dependent lifetime curves of the samples from each group after the superacid-derived passivation are shown in Fig. 1 (a). As can be seen, the lifetime of the degraded sample (Group D) is two orders of magnitude lower than the as grown sample (Group N) and the defect-annihilated sample (Group A) across the entire measured injection range. This indicates the effective lifetime of the degraded sample is dominated by the recombination lifetime of the activated bulk defects.

The room temperature photoluminescence (PL) image of the degraded sample after the superacid-derived passivation is shown in Fig. 1(b). The PL counts at the center of the wafer is much lower than the PL counts at the periphery, indicating that the activated defects have a non-uniform spatial distribution. This characteristic agrees with previous studies of these thermally activated defects in FZ silicon.[8,9] In this study, the lifetime curves and DLTS spectra of the degraded samples are all measured from the center.

The room temperature lifetime curves of the degraded sample with a-Si passivation before and after the TIDLS measurements are also shown in Fig. 1(a). These two lifetime curves are similar to the lifetime curve of the degraded sample with a superacid-derived passivation, indicating (a) the a-Si layer provides surface passivation quality that is sufficient for the effective lifetime of the degraded sample to be dominated by the activated bulk defects; (b) the thermally activated defects were not impacted by the deposition process of the a-Si layer; and (c) the thermally activated defects were not impacted by the TIDLS measurements.

Electrical Characterization of the Defects

The electrical properties of the thermally activated defects are investigated by a combination of DLTS and TIDLS. The measured DLTS spectra are shown in Fig. 2. No clear electron emission signals are detected in the spectra of the as-grown sample (Group N) or the defect-annihilated (Group A) sample. In the DLTS spectrum of the degraded sample (Group D), four distinguished peaks can be observed. With a Laplace-DLTS analysis,[10] it was found that the peak at around 180 K consists of contributions from two electron emission signals. The activation energies for electron emission from the observed traps, E_1-E_5, have been determined as 0.16±0.005, 0.20±0.005, 0.28±0.005, 0.405±0.01 and 0.43±0.01 eV, respectively. These defect levels are similar to the ones identified by Grant *et al.*[8] In the degraded samples studied by Grant *et al.*[8], the E_3 center had the highest concentration among all the traps, whereas according to our results the E_4 and E_5 traps have higher concentrations. In either case, it is unclear which level is most responsible for the dramatic decrease of lifetime.

By changing the filling pulse length in the DLTS measurements, it was found that the electron capture cross sections σ_n of the E_1, E_2, E_3 and E_4 traps are larger than 10^{-16} cm^2 with weak (if any) temperature dependence, whereas σ_n of the E_5 trap shows an exponential growth with temperature according to the following equation, $\sigma_n = 7\times10^{-16}\exp(-0.19/kT)$ cm^2. Minority carrier transient spectroscopy (MCTS) measurements were also performed; yet, no hole emission signal from a defect level in the lower half of the bandgap was observed.

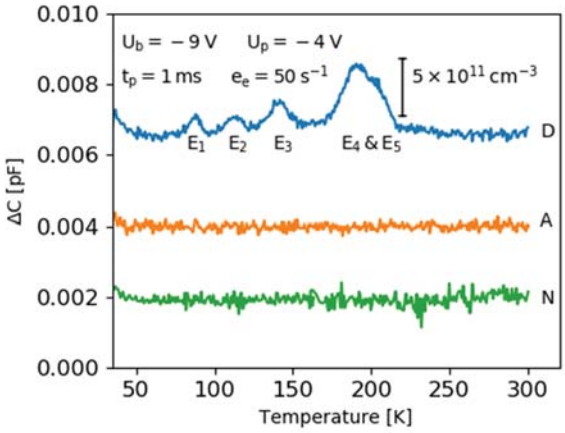

FIGURE 2. DLTS spectra of one sample from each group. The spectra are shifted for clarity. The measurement settings are shown in the graph. U_b and U_p are the reverse bias voltage and filling pulse voltage respectively, t_p is the filling pulse length and e_e is the electron emission rate.

In order to quantify the recombination activity of the activated defects, TIDLS measurements were performed on the as-grown, degraded and annealed samples. For all temperatures, the lifetimes of control samples and defect-annihilated samples are nearly two orders of magnitude higher than the lifetimes of the degraded samples. Therefore, the impact of surface recombination and intrinsic recombination on the effective lifetime of the degraded samples can be considered as negligible. In our TIDLS analysis, we still use the inversely subtracted lifetime $(1/\tau_D - 1/\tau_A)^{-1}$ to further minimize the impact of surface and intrinsic recombination, where τ_D and τ_A are the lifetime of the degraded sample and defect-annihilated sample respectively. In Fig. 3(a), the inversely subtracted lifetimes of the degraded sample are shown for different temperatures.

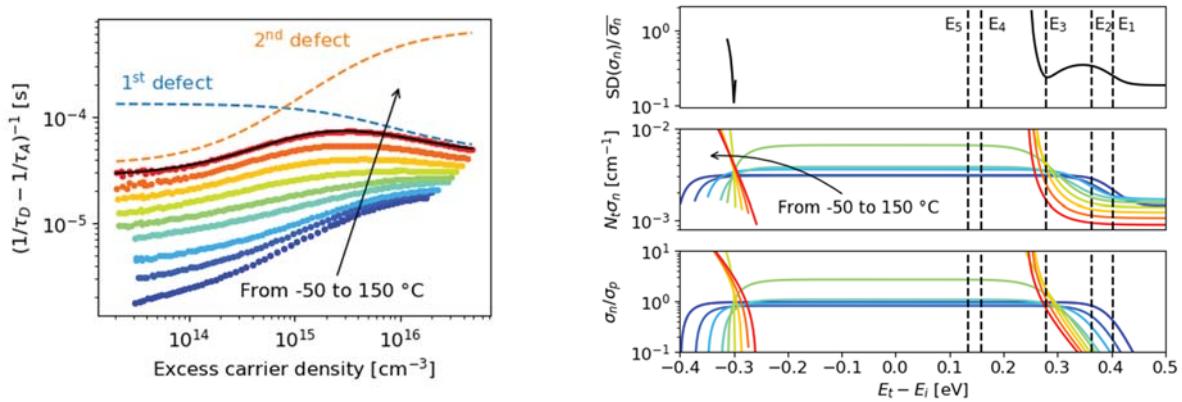

(a) (b)

FIGURE 3. (a) Inversely subtracted lifetime $(1/\tau_D - 1/\tau_A)^{-1}$ from −50 °C to 150 °C, as well as a two defects fitting of the lifetime at 150 °C. (b) DPSS curves resulted from the TIDLS measurements.

The inversely subtracted lifetimes are then fitted with Shockley-Read-Hall statistics[18,19] using the method described in Murphy *et al.*[20] and Morishige and Jensen *et al.*[21] It was found that at least two defect levels are required to achieve a satisfactory fitting of the measured data. In Fig. 3(a), the fitting of the lifetime at 150 °C is shown. At each temperature, the best fitted lifetime curve can be reproduced by infinite combinations of defect parameters (energy level E_t and the productions of defect density N_t and the two capture cross sections σ_n and σ_p). These infinite combinations can be represented by the so-called defect parameter solution surface (DPSS) curve.[13] Since for most of the measured temperatures, the 2st defect dominates the lifetime only at a narrow injection range, the uncertainty of analyzing the 2nd defect can be large. Hence, here we focus only on the analysis of the 1st defect. The DPSS curves for the 1st defect at each temperature are shown in the bottom two graphs of Fig. 3(b). Each curve in these two graphs represents the infinite combinations of the E_t, $N_t \cdot \sigma_n$ and σ_n/σ_p that can best fit the lifetime curve at that temperature. If it is assumed that σ_n is temperature independent, then all the DPSS curves for $N_t \cdot \sigma_n$ (middle figure) should intersect at the true E_t of the defect. In the upper graph of Fig. 3(b), the standard deviation of σ_n normalized by their mean value is plotted. The black dashed lines in Fig. 3(b) represent the five defect levels identified by DLTS. As can be seen, the level E_3 (0.28±0.005 eV) coincides with a local minimum in the standard deviation curve. Since σ_n of E_3 was found to be temperature independent by DLTS, this indicates that E_3 is likely to be the most dominating defect level at room temperature. From the DPSS curve for σ_n/σ_p (the bottom subfigure), the capture cross section ratio of this defect level at room temperature is around 0.88±0.09. Meanwhile, another local minimum of the standard deviation curve can be identified in the lower half of the bandgap. However, this defect level has not been detected by MCTS measurements.

Hydrogenation of the Activated Defects

The room temperature lifetime curves of a degraded sample (Group D) and a defect-annihilated sample (Group A) are shown in Fig. 4. The lifetime of the degraded sample with a-Si passivation is also shown for comparison. As can be seen, after SiN_x deposition, the lifetime of the degraded sample has increased by one order of magnitude. Since the effective lifetime of the degraded sample with a-Si passivation is dominated by the thermally activated bulk defects, this increase of lifetime indicates that some of the activated defects has been passivated during the SiN_x deposition. Note that the deposition temperature is around 425 °C, which is in the range that the defects are

activated. Therefore, the passivation is not likely to be a result of a thermal effect. Instead, this passivation is likely resulted from the hydrogenation effect induced during the PECVD process. Similar results have also been found by Rougieux *et al.*[22]

After SiN_x passivation, the lifetime of the degraded sample is still much lower than the lifetime of the defect-annihilated sample, indicating that the hydrogenation occur in the PECVD process cannot fully passivate the activated bulk defects. Therefore, even if the *n*-type FZ silicon will be passivated by hydrogen rich SiN_x film, the impact of the thermally activated defects still needs to be considered if the sample needs to be annealed in the temperature range leads to degradation.

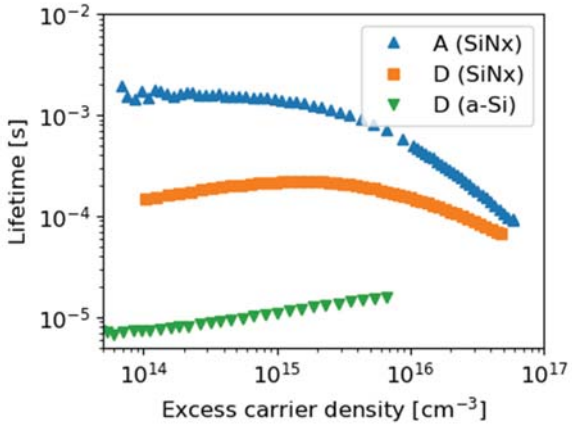

FIGURE 4. Room temperature lifetime curves for a defect-annihilated sample ("A") and a degraded sample ("D") passivated with SiN_x as well as the lifetime of the degraded sample passivated with a-Si.

CONCLUSIONS

FZ silicon should not be intuitively considered as bulk defect free or stable material. Annealing at 500 °C results in the formation of recombination active defects in *n*-type FZ silicon. These thermally activated defects can decrease the lifetime of the sample by more than two orders of magnitude. Using a combination of DLTS and TIDLS, we identified that the most recombination active defect level among the thermally activated defect levels is located at 0.28±0.005 eV below the conduction band, with a capture cross section ratio of 0.88±0.09 at room temperature. The effect of hydrogenation on the thermally activated defect is investigated by depositing a hydrogen rich SiN_x film on the degraded sample. It has been found that the thermally activated defects can be partially passivated solely from the hydrogenation occurring during the deposition (no additional firing).

ACKNOWLEDGMENTS

This work was supported by the Australian Government through the Australian Renewable Energy Agency under grant ARENA 2017/RND001. The views expressed herein are not necessarily the views of the Australian Government, and the Australian Government does not accept responsibility for any information or advice contained herein. Work at Warwick and Manchester was supported by the EPSRC SuperSilicon PV project (EP/M024911/1).

REFERENCES

1. J. Zhao, A. Wang, M.A. Green, and F. Ferrazza, Appl. Phys. Lett. **73**, 1991 (1998).
2. A. Richter, J. Benick, F. Feldmann, A. Fell, M. Hermle, and S.W. Glunz, Sol. Energy Mater. Sol. Cells **173**, 96 (2017).
3. M.A. Jensen, A. Zuschlag, S. Wieghold, D. Skorka, A.E. Morishige, G. Hahn, and T. Buonassisi, J. Appl. Phys. **124**, 085701 (2018).
4. C. Sun, H.T. Nguyen, H.C. Sio, F.E. Rougieux, and D. Macdonald, IEEE J. Photovoltaics **7**, 988 (2017).
5. T. Lauinger, J. Schmidt, A.G. Aberle, and R. Hezel, Appl. Phys. Lett. **68**, 1232 (1996).

6. B. Hoex, S.B.S. Heil, E. Langereis, M.C.M. van de Sanden, and W.M.M. Kessels, Appl. Phys. Lett. **89**, 042112 (2006).
7. A. Richter, S.W. Glunz, F. Werner, J. Schmidt, and A. Cuevas, Phys. Rev. B **86**, 165202 (2012).
8. N.E. Grant, V.P. Markevich, J. Mullins, A.R. Peaker, F. Rougieux, and D. Macdonald, Phys. Status Solidi - Rapid Res. Lett. **10**, 443 (2016).
9. N.E. Grant, V.P. Markevich, J. Mullins, A.R. Peaker, F. Rougieux, D. Macdonald, and J.D. Murphy, Phys. Status Solidi **213**, 2844 (2016).
10. J. Mullins, V.P. Markevich, M. Vaqueiro-Contreras, N.E. Grant, L. Jensen, J. Jabłoński, J.D. Murphy, M.P. Halsall, and A.R. Peaker, J. Appl. Phys. **124**, 035701 (2018).
11. D. Sperber, A. Herguth, and G. Hahn, Phys. Status Solidi - Rapid Res. Lett. **11**, 1600408 (2017).
12. T. Niewelt, M. Selinger, N.E. Grant, W. Kwapil, J.D. Murphy, and M.C. Schubert, J. Appl. Phys. **121**, 185702 (2017).
13. S. Rein, *Lifetime Spectroscopy: A Method of Defect Characterization in Silicon for Photovoltaic Applications* (Springer Science and Business Media, Berlin, 2006).
14. S. Bernardini, T.U. Norland, G. Coletti, L. Ding, A.L. Blum, and M.I. Bertoni, in *43rd IEEE Photovolt. Spec. Conf.* (IEEE, 2016), pp. 2863–2867.
15. N.E. Grant, T. Niewelt, N.R. Wilson, E.C. Wheeler-Jones, J. Bullock, M. Al-Amin, M.C. Schubert, A.C. Van Veen, A. Javey, and J.D. Murphy, IEEE J. Photovoltaics **7**, 1574 (2017).
16. R.A. Sinton, A. Cuevas, and M. Stuckings, in *25th IEEE Photovolt. Spec. Conf.* (IEEE, 1996), pp. 457–460.
17. Z. Hameiri, N. Borojevic, L. Mai, N. Nandakumar, K. Kim, and S. Winderbaum, IEEE J. Photovoltaics **7**, 996 (2017).
18. W. Shockley and W.T. Read, Phys. Rev. **87**, 835 (1952).
19. R.N. Hall, Phys. Rev. **87**, 387 (1952).
20. J.D. Murphy, K. Bothe, R. Krain, V. V Voronkov, and R.J. Falster, J. Appl. Phys. **111**, 113709 (2012).
21. A.E. Morishige, M.A. Jensen, D.B. Needleman, K. Nakayashiki, J. Hofstetter, T.A. Li, and T. Buonassisi, IEEE J. Photovoltaics **6**, 1466 (2016).
22. F.E. Rougieux, N.E. Grant, C. Barugkin, D. Macdonald, and J.D. Murphy, IEEE J. Photovoltaics **5**, 495 (2015).